Received: 5 July 2019 | Revised: 30 August 2019 | Accepted: 2 September 2019

DOI: 10.1002/bit.27166

ARTICLE

BIOTECHNOLOGY BIOENGINEERING WILEY

From three-dimensional morphology to effective diffusivity in filamentous fungal pellets

Stefan Schmideder[1] | Lars Barthel[2] | Henri Müller[1] | Vera Meyer[2] | Heiko Briesen[1]

[1]Chair of Process Systems Engineering, Technical University of Munich, Freising, Germany

[2]Department of Applied and Molecular Microbiology, Institute of Biotechnology, Technische Universität Berlin, Berlin, Germany

Correspondecne
Heiko Briesen, Technical University of Munich, Chair of Process Systems Engineering, 85354 Freising, Germany.
Email: heiko.briesen@tum.de

Funding information
Deutsche Forschungsgemeinschaft, Grant/Award Number: 198187031, 315305620,315384307

Abstract

Filamentous fungi are exploited as cell factories in biotechnology for the production of proteins, organic acids, and natural products. Hereby, fungal macromorphologies adopted during submerged cultivations in bioreactors strongly impact the productivity. In particular, fungal pellets are known to limit the diffusivity of oxygen, substrates, and products. To investigate the spatial distribution of substances inside fungal pellets, the diffusive mass transport must be locally resolved. In this study, we present a new approach to obtain the effective diffusivity in a fungal pellet based on its three-dimensional morphology. Freeze-dried *Aspergillus niger* pellets were studied by X-ray microcomputed tomography, and the results were reconstructed to obtain three-dimensional images. After processing these images, representative cubes of the pellets were subjected to diffusion computations. The effective diffusion factor and the tortuosity of each cube were calculated using the software GeoDict. Afterwards, the effective diffusion factor was correlated with the amount of hyphal material inside the cubes (hyphal fraction). The obtained correlation between the effective diffusion factor and hyphal fraction shows a large deviation from the correlations reported in the literature so far, giving new and more accurate insights. This knowledge can be used for morphological optimization of filamentous pellets to increase the yield of biotechnological processes.

KEYWORDS

Aspergillus niger, effective diffusion, filamentous fungal pellets, tortuosity, X-ray microcomputed tomography

1 | INTRODUCTION

Filamentous fungi are widely used cell factories for the production of a variety of compounds such as enzymes, organic acids, or antibiotics (Meyer, 2008). As just one example, plant-biomass-degrading enzymes produced by filamentous fungi, have a global market value of € 4.7 billion (Meyer et al., 2016). During submerged cultivation, filamentous fungi adopt different macromorphological entities such as non-aggregated hyphae (disperse mycelia), loosely aggregated hyphal clumps, and densely aggregated spherical structures (pellets; Pirt, 1966). This morphology is influenced by the fungal species and cultivation parameters (Papagianni, 2004). Depending on the predominant morphology in a submerged fungal culture, the substances produced by the organism can differ significantly. As fungal growth and protein secretion are coupled processes, it is for example known that the highest protein secretion normally occurs during rapid hyphal growth, which takes place in disperse mycelia and the outer layers of fungal pellets where nutrient supply is not limited (Cairns, Zheng, Zheng, Sun, & Meyer, 2019). On the

other hand, the production of secondary metabolites peaks when the producing organism shows an extremely low or zero growth (Brakhage, 2013). These conditions can be observed for example in the dense center of fungal pellets, where the restricted diffusion of oxygen and nutrients leads to limitations, thus inhibiting growth (Veiter, Rajamanickam, & Herwig, 2018). This demonstrates that a detailed understanding of the limitations and diffusion processes in fungal pellets is of crucial importance for many biotechnological applications.

The effective diffusion coefficient is required to calculate the diffusive mass transport. For component i in a porous medium, this parameter can be expressed as (Becker, Wieser, Fell, & Steiner, 2011)

$$D_{i,\mathrm{eff}} = D_{i,\mathrm{bulk}} \cdot k_{\mathrm{eff}}, \tag{1}$$

where $D_{\mathrm{i,bulk}}$ is the diffusion coefficient of component i in the bulk medium without geometrical hindrance and k_{eff} describes the reduction of the free bulk diffusion $D_{\mathrm{i,\,bulk}}$ to the effective diffusion $D_{\mathrm{i,\,eff}}$ and is solely dependent on the pore geometry and independent of the diffusing substance i (Becker et al., 2011). Hereafter, k_{eff} is called the effective diffusion factor. In the case of diffusion in filamentous pellets, $D_{\mathrm{i,\,bulk}}$ corresponds to the molecular diffusion coefficient of components such as oxygen, glucose, or products in the fermentation medium and is strongly dependent on the medium, diffusing substance, and process conditions such as temperature. Temperature-dependent bulk diffusion coefficients for glucose, oxygen, and several other compounds in aqueous solutions can be estimated, for example, from Yaws (2014). The geometrically caused reduction of the diffusion, k_{eff}, can be expressed as (Epstein, 1989):

$$k_{\mathrm{eff}} = \frac{\epsilon}{\tau^2}, \tag{2}$$

where the porosity, ϵ, is defined as the ratio of volume of voids to the total volume. The tortuosity, τ, is a geometrical parameter and can be taken as the ratio of the average pore length to the length of the porous medium along the major flow or diffusion axis. Thus, in general it is > 1 (Epstein, 1989).

So far, no experimental or modeling approaches to exactly predict the diffusive mass transport inside whole fungal pellets are available. Several modeling approaches of filamentous microorganisms consider the diffusive mass transport of oxygen and/or substrates like glucose (Buschulte, 1992; Celler, Picioreanu, van Loosdrecht, & van Wezel, 2012; Cui, Van der Lans, & Luyben, 1998; Lejeune & Baron, 1997; Meyerhoff, Tiller, & Bellgardt, 1995; Table 1). They include effective diffusion coefficients that are dependent on the molecular

TABLE 1 Applied correlations between effective diffusion coefficients ($D_{\mathrm{i,eff}}$), effective diffusion factor (k_{eff}), bulk diffusion coefficients ($D_{\mathrm{i,bulk}}$), porosity (ϵ), hyphal fraction ($c_{\mathrm{h}} = 1 - \epsilon$), solid fraction ($\phi$), and tortuosity ($\tau$) in the literature to model the diffusive transport mechanisms

Eq. for k_{eff} in $D_{i,\mathrm{eff}} = D_{i,\mathrm{bulk}} k_{\mathrm{eff}}$	Origin structure	Diffusion direction	Field	Source
$1 - c_{\mathrm{h}}$	–	–	Filamentous microorganisms	Celler et al. (2012)
	–	–	Filamentous microorganisms	Cui et al. (1998) adopted from Van't Riet and Tramper (1991)
	–	–	Filamentous microorganisms	Buschulte (1992) adopted from Aris (1975)
$\frac{(1-c_{\mathrm{h}})}{\tau}$ with $\tau = 2$	–	–	Filamentous microorganisms	Lejeune and Baron (1997)
$\frac{2-2c_{\mathrm{h}}}{2+c_{\mathrm{h}}}$	–	–	Filamentous microorganisms	Meyerhoff et al. (1995) adopted from Neale and Nader (1973)
$\exp(-2.8c_{\mathrm{h}})$	–	–	Filamentous microorganisms	Buschulte (1992) adopted from Vorlop (1984)
$\left(1 - \frac{2\phi}{1+\phi-\frac{0.30583\,\phi^4}{1-1.40296\,\phi^8}-0.01336\,\phi^8}\right)$	–	Perpendicular to fibers	Square array of parallel fibers	Perrins et al. (1979)
$\frac{\epsilon}{\tau^2}$ with $\tau^2 = \exp(1.16(1-\epsilon))$	Simulated	Perpendicular to fibers	Nonoverlapping parallel fibers	Tomadakis and Sotirchos (1993), Tomadakis and Robertson (2005)
$\frac{\epsilon}{\tau^2}$ with $\tau^2 = \left(\frac{1-0.33}{\epsilon-0.33}\right)^{0.707}$	Simulated	Perpendicular to fibers	Overlapping parallel fibers	Tomadakis and Sotirchos (1991)
$\frac{\epsilon}{\tau^2}$ with $\tau^2 = \left(\frac{1-0.04}{\epsilon-0.04}\right)^{0.107}$	µCT	Parallel to fibers	Parallel carbon fibers	Vignoles et al. (2007)
$\frac{\epsilon}{\tau^2}$ with $\tau^2 = \left(\frac{1-0.04}{\epsilon-0.04}\right)^{0.465}$	µCT	Perpendicular to fibers	Parallel carbon fibers	Vignoles et al. (2007)
$\frac{\epsilon}{\tau^2}$ with $\tau^2 = \left(\frac{1-0.037}{\epsilon-0.037}\right)^{0.661}$	Simulated	All directions	Overlapping nonparallel fibers	Tomadakis and Sotirchos (1991)
$1.05\epsilon^3$	Simulated	All directions	Overlapping nonparallel fibers	He et al. (2017)

diffusion coefficient, tortuosity, and porosity/hyphal fraction. Thereby, the hyphal fraction, $c_h = 1 - \epsilon$, is defined as the ratio of the volume of hyphae to the total volume. It is important to note that the modeling approaches published so far (Buschulte, 1992; Celler et al., 2012; Cui et al., 1998; Lejeune & Baron, 1997; Meyerhoff et al., 1995) either neglect the tortuosity of the hyphal structure or assume a constant tortuosity for different porosities. These simplifications may be caused by the absence of information about the tortuosity. In the materials science of fibers, correlations between the porosity and the effective diffusion factor for bulk diffusion that include knowledge about the tortuosity have been described. Perrins, McKenzie, and McPhedran (1979) derived an analytic expression for ideal square arrays of parallel fibers, Tomadakis and Sotirchos (1991) a correlation for random distributed overlapping parallel fibers, Tomadakis and Sotirchos (1993) and Tomadakis and Robertson (2005) a relation for random distributed nonoverlapping parallel fibers, Tomadakis and Sotirchos (1991) and He, Guo, Li, Pan, and Wang (2017) a relation for 3D random distributed overlapping fibers, and Vignoles, Coindreau, Ahmadi, and Bernard (2007) a correlation for parallel fibrous carbon–carbon composite preforms (Table 1). The only published experimental approach to predict the diffusive mass transport is based on the measurement of oxygen concentrations using microelectrodes inside fungal pellets (Hille, Neu, Hempel, & Horn, 2009; Wittier, Baumgartl, Lübbers, & Schügerl, 1986). The researchers correlated the mass transport of oxygen into the pellets with microscopic information from cryo-slices. However, the microscopy images of the cryo-slices missed the three-dimensional information of the hyphal network and hyphae superimposed in the two-dimensional projections. Therefore, the appropriate correlation between pellet morphology and diffusion was not possible in this experimental approach. We could recently overcome the limitations of two-dimensional image generation by performing X-ray microcomputed tomography (μCT) measurements on whole fungal pellets (Schmideder et al., 2019). The investigated *Aspergillus niger* pellet showed a very complex three-dimensional structure. With a diameter of 633 μm, the *A. niger* pellet had a hyphal length of 1.5 m and 15,425 tips in total.

In materials science, μCT measurements and subsequent mass-transfer computations matured into a widely used method to determine the effective diffusivity of porous/fibrous materials. Exemplarily, Panerai et al. (2017), Becker et al. (2011), Coindreau, Mulat, Germain, Lachaud, and Vignoles (2011), and Foerst et al. (2019) investigated the effective diffusivity of fibrous insulators, fuel cell media, carbon-carbon composites, and maltodextrin solutions, respectively. Thereby, μCT appeared as a non-destructive technique to measure three-dimensional microstructures.

In this study, we computed the effective diffusivity of *A. niger* pellets based on the micro-structural characterization gained from μCT measurements and subsequent image analysis. The newly developed technique for fungal pellets combines the experimental acquisition of three-dimensional images with the locally resolved calculation of the effective diffusion coefficient and tortuosity within this structure for the first time. This results in an unprecedented potential for the determination of diffusion processes inside fungal pellets.

2 | MATERIALS AND METHODS

2.1 | Preparation of pellets

The *A. niger* hyperbranching strain MF22.4, which has been shown to be a better protein-secretion strain than the wild-type strain (due to deletion of the racA gene; Fiedler, Barthel, Kubisch, Nai, & Meyer, 2018), was used in this study. Pellets were obtained by submerged cultivation of MF22.4 for 48 hr and freeze-drying following the previously described protocol (Schmideder et al., 2019).

2.2 | X-ray microcomputed tomography

To obtain three-dimensional images of the freeze-dried filamentous pellets, μCT measurements were performed based on the method reported by Schmideder et al. (2019). Two-dimensional projections from different angles were reconstructed to generate three-dimensional images with a custom-designed software (Matrix Technologies, Feldkirchen, Germany) that uses CERA (Siemens, Munich, Germany). The image resolution was 1 μm (i.e., the edge length of the voxels was 1 μm), and to generate the beam, 60 kV and 25 μA were applied. Depending on the size of the pellets, 1-5 pellets can be measured with one μCT-measurement (3 hr including the time for image reconstruction). An instant adhesive (UHU, Bühl, Germany) was used to fix the freeze-dried fungal pellets on top of a sample holder. In contrast to the previous study (Schmideder et al., 2019), in this case, the instant adhesive dried 5 min before placing the pellets on top of the holder. This procedure resulted in a smooth surface of the instant adhesive, while it remained sticky enough to fix the pellets. The smooth surface facilitated the segmentation of the instant adhesive in the subsequent image processing.

2.3 | Image processing

Image processing aimed at differentiating between hyphal material and background. The background included the instant adhesive used for sample fixation, the air between the hyphae, and small impurities. In general, image processing is leaned to the one reported in the section "Preprocessing" by Schmideder et al. (2019)). The image processing result for one pellet is exemplarily illustrated in Figure 1.

As the instant adhesive showed similar gray values as the pellets, we did not implement an automated segmentation. Instead, the instant adhesive at the bottom of the pellets was cropped manually using the commercial software VGSTUDIO MAX (version 3.2, Volume Graphics GmbH, Heidelberg, Germany) in a first processing step. The further image processing steps were carried out automatically using MATLAB (version 2018a, MathWorks, Natick, MA). To differentiate between hyphae and air voxels, a threshold – calculated by Otsu's method (Otsu, 1979) – was applied on the gray value images. Finally, small connected objects with a maximum size of 1,000 μm^3 were deleted to eliminate objects that were not part of the pellet. The processed three-dimensional pellets were used for further diffusion computations.

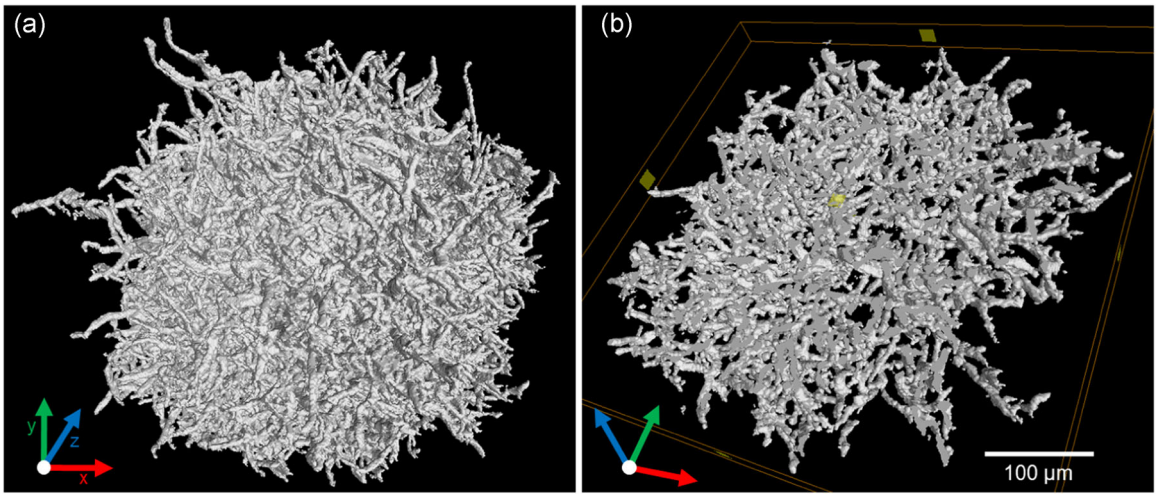

FIGURE 1 Processed three-dimensional µCT image of an *Aspergillus niger* pellet. The images were rendered using VGSTUDIO MAX. (a) Projection of the whole pellet. (b) Projection of a central slice with a depth of 25 µm [Color figure can be viewed at wileyonlinelibrary.com]

2.4 | Representative cubes for diffusion computations of *A. niger* pellets

To compute the spatially resolved effective diffusivity in fungal pellets, we extracted representative cubic sub-volumes of the processed three-dimensional images. The diffusive mass transport was computed, as described in Section 2.6 using these cubes. The centers of the cubes used for diffusion computations were selected along the main axis originating from the calculated mass center of the *A. niger* pellets. The distance between the centers of the cubes along the main axis was set to 25 µm. In Figure 2, the distance between the cubes was increased for the sake of clarity. To identify the influence of the cube-size on the diffusion computations, the edge length of the cubes was varied to 30, 50, 70, and 90 µm.

2.5 | Beam-Pellet

A common assumption for the effective diffusion coefficient of filamentous microorganisms is the direct proportionality to the porosity ϵ (Buschulte, 1992; Celler et al., 2012; Cui et al., 1998; Silva, Gutierrez, Dendooven, Hugo, & Ochoa-Tapia, 2001):

$$D_{i,\mathrm{eff}} = D_{i,\mathrm{bulk}} \cdot \epsilon. \tag{3}$$

Thereby, the effective diffusion factor k_{eff} is assumed to be equal to the porosity, and the tortuosity is neglected. To imitate a filamentous spherical object, where the tortuosity can be nearly neglected, we simulated a so-called "Beam-Pellet," which was used to validate the

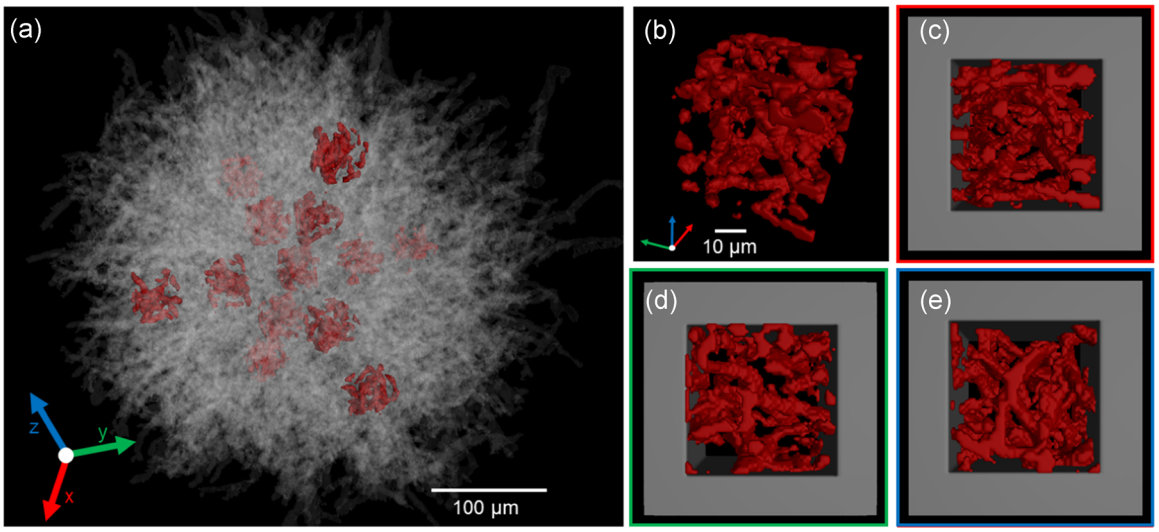

FIGURE 2 Processed three-dimensional µCT image of the *Aspergillus niger* pellet of Figure 1 and cubes for the diffusion computations: (a) Transparent: projection of a whole pellet; red: exemplary cubes that were used for the diffusion computations. (b–e) Morphology of a single cube from different viewing directions; the gray boundaries in (c–e) illustrate the boundaries parallel to the diffusion computation. (b) Cube without illustration of boundaries for the diffusion computations. (c) Cube for diffusion in the *x*-direction. (d) Cube for diffusion in the *y*-direction. (e) Cube for diffusion in the z-direction [Color figure can be viewed at wileyonlinelibrary.com]

method of the diffusion computation and critically scrutinize the tortuosity neglect in the literature.

The "Beam-Pellet" (Figure 3) was built up from equally sized filaments (in diameter and length) with their origin in the pellet center and having a radial orientation. To guarantee a uniform distribution of the filaments in space, their orientation was calculated using the HEALPIx (hierarchical equal area iso-latitude pixelization) discretization (Gorski et al., 2005). In this way, 50,700 representative, equally distributed points were calculated on the pellet surface; all of them were connected to the pellet center. Then, the connected lines were dilated with MATLAB to obtain a "Beam-Pellet" with a defined diameter of the filaments. The diameter was chosen to be 3 μm, similar to the average hyphal diameter of *A. niger* (Colin, Baigorí, & Pera, 2013; Nielsen, 1993; Schmideder et al., 2019). To investigate the influence of the image resolution on the subsequent diffusion computations, similar "Beam-Pellets" with different resolutions were simulated. Starting from a "Beam-Pellet" with a radius of 700 voxels and a dilation of one voxel, the resolution of the filaments was increased. Thereby, the number of filaments was kept constant, whereas the radius of the "Beam-Pellet" was set to 1,167, 1,633, 2,567, and 3,500 voxels and the dilation was set to 2, 3, 5, and 7 voxels, respectively. Thus, the "Beam-Pellets" only differed in the scaling and the resolution of the filaments. The effective diffusivity of the "Beam-Pellet" was analyzed, as described in Section 2.6. This analysis required cubes that represent the whole pellet. Similar to the case of the *A. niger* pellets, cubes located along the main axes were chosen to investigate the effective diffusivity (Figure 3). Identical to the final analysis of the *A. niger* pellets, the cube-edge length was set to 50 μm, and the cubes were selected along the main axis. Thus, the cube edge length was 50 voxels for the "Beam-Pellet" with a radius of 700 voxels and a dilation of one voxel. To guarantee that the same structure (50 μm × 50 μm × 50 μm) was analyzed for higher resolutions, we increased the cube edge length to 83, 117, 183, and 250 voxels, respectively. In Figure 4, the same representative cube is shown for different resolutions.

2.6 | Computation of the effective diffusivity

To compute the effective diffusion factor and tortuosity of filamentous structures (Equation (2)), the module DiffuDict of the commercial software GeoDict (Becker et al., 2011; Velichko, Wiegmann, & Mücklich, 2009; Wiegmann & Zemitis, 2006; Math2Market Gmbh, Kaiserslautern, Germany) was used. As DiffuDict allows for the voxel-based solution of transport equations, the processed three-dimensional image data of the μCT measurements as well as the simulated "Beam-Pellet," could be used for the diffusion computations. DiffuDict requires cubic domains for the diffusion computations, and therefore, cubic sub-volumes of the filamentous pellets were extracted from the three-dimensional images for further analysis. The selections of representative sub-volumes are described in Sections 2.4 and 2.5 for *A. niger* pellets and the "Beam-Pellet," respectively. Conceptually, as shown in Figures 2c–e and 3c–e, the diffusion computations in DiffuDict were executed in one of the three main axes for each computation. As the representative cubes were chosen along the main axes, we were able to apply three computations on each cube and could thus analyze the effective diffusivity of each cube in the radial and in two tangential directions. The computational effort to obtain the diffusivity of one cube in the three directions was about 1 min for cubes with 50 × 50 × 50 voxels with an Intel Xeon E5-1660 CPU (3.7 GHz). The details of the computations are described in the following.

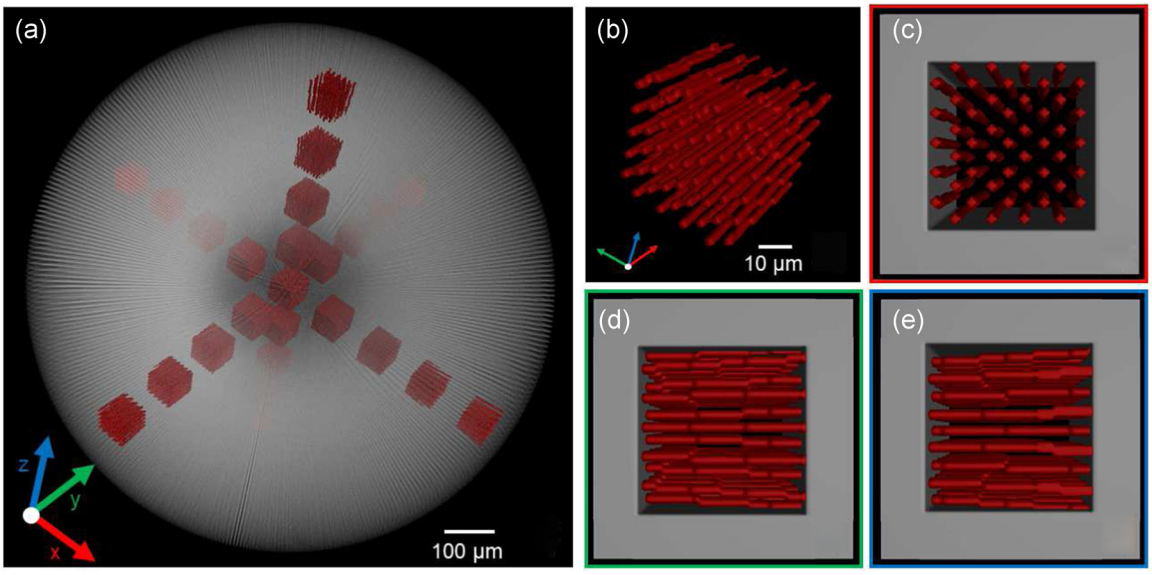

FIGURE 3 Simulated "Beam-Pellet" and cubes for diffusion computations: (a) Transparent: projection of the whole pellet; red: exemplary cubes that were used for the diffusion computations. (b–e) Morphology of a single cube from different viewing directions; the gray boundaries in (c–e) illustrate the boundaries parallel to the diffusion computation. (b) Cube without illustration of boundaries for the diffusion computations. (c) Cube for diffusion in the *x*-direction. (d) Cube for diffusion in the *y*-direction. (e) Cube for diffusion in the *z*-direction [Color figure can be viewed at wileyonlinelibrary.com]

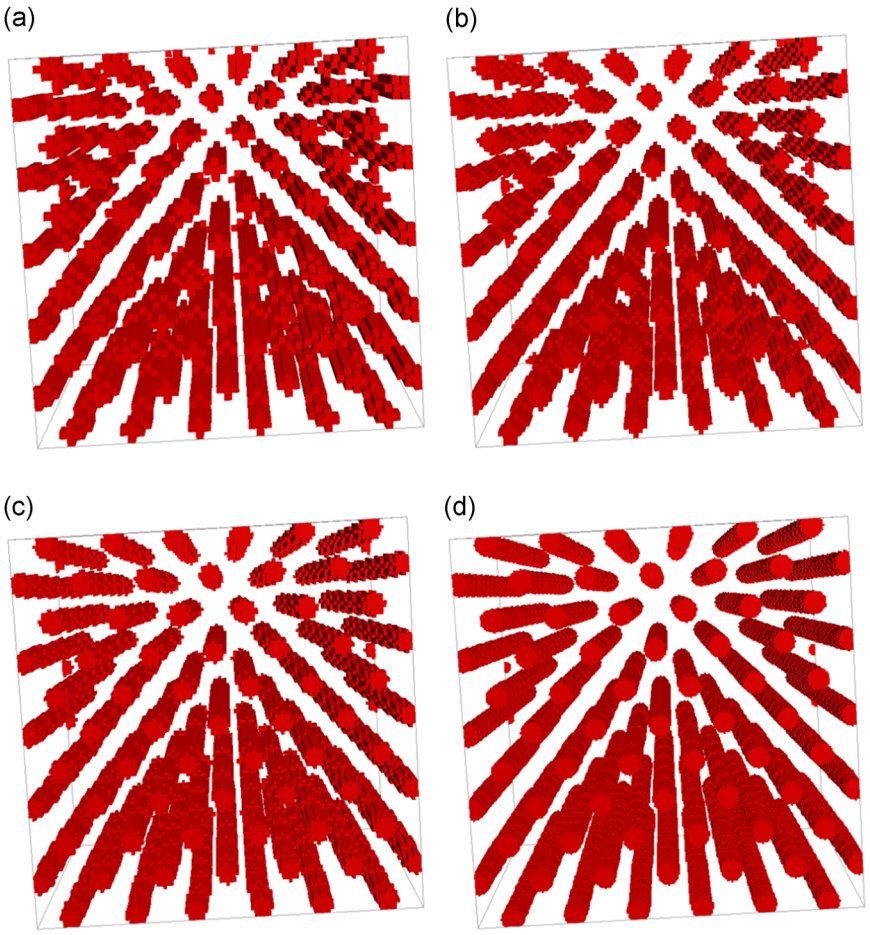

FIGURE 4 Same representative cube of "Beam-Pellets" with different resolutions: (a) Three voxels per filament (dilation 1). (b) Five voxels per filament (dilation 2). (c) Seven voxels per filament (dilation 3). (d) 15 voxels per filament (dilation 7) [Color figure can be viewed at wileyonlinelibrary.com]

We computed the diffusion in the space/liquid between the hyphae (porous medium). The predominant diffusion regime in liquids is bulk diffusion (Becker et al., 2011; Panerai et al., 2017), that is, mass transport is mainly driven by collisions between fluid molecules. In our approach, we neglected surface effects on the solid–liquid interface that could influence diffusion. One possible effect could be surface diffusion, that is molecules can diffuse on the surface of pores. This phenomenon is known to be an important transport mechanism in reversed-phase liquid chromatography. However, predictions are difficult and depend on the temperature, surface concentration, and surface chemistry (Medveď & Černỳ, 2011; Miyabe & Guiochon, 2010). Electrical double-layers on solid–liquid interfaces could change the diffusivity through porous media, especially the diffusivity of ions (Gabitto & Tsouris, 2017). In the present study we assumed pure bulk diffusion. In the case of pure bulk diffusion, the diffusion in the pores can be modeled by the Laplace equation, with Neumann boundary conditions on the pores-to-solids boundaries and a concentration drop of the diffusing component in the diffusion direction (Becker et al., 2011). Thus, we applied bulk diffusion in DiffuDict and applied a concentration drop of the diffusing component between the inlet and outlet. To avoid a bias in the diffusion computations, we chose Dirichlet boundary conditions on the in- and outlet and symmetric boundary conditions on the other four faces. Computing the total diffusion flux through the porous structures and applying Fick's law, DiffuDict calculates the effective diffusion factor (Becker et al., 2011; Wiegmann & Zemitis, 2006). According to Equation (2), the tortuosity can be calculated from the porosity and the effective diffusion factor. Therefore, both the effective diffusion factor and the tortuosity were calculated for each representative sub-volume of the filamentous pellets.

3 | RESULTS AND DISCUSSION

3.1 | Effective diffusivity of the "Beam-Pellet"

The "Beam-Pellet" introduced in Section 2.5 (Figure 3) imitates a hypothetical filamentous pellet that grew only in the radial direction and is similar but not identical to parallel fibers. We compared the diffusion behavior of the "Beam-Pellet" with literature correlations for the diffusion through parallel fibers to validate the diffusion computations. Additionally, we critically scrutinized the literature assumption that $k_{\text{eff}} = \epsilon$ (Buschulte, 1992; Celler et al., 2012; Silva et al., 2001; Van't Riet & Tramper, 1991), where the tortuosity is neglected and the effective diffusion factor is assumed to be only dependent on the porosity.

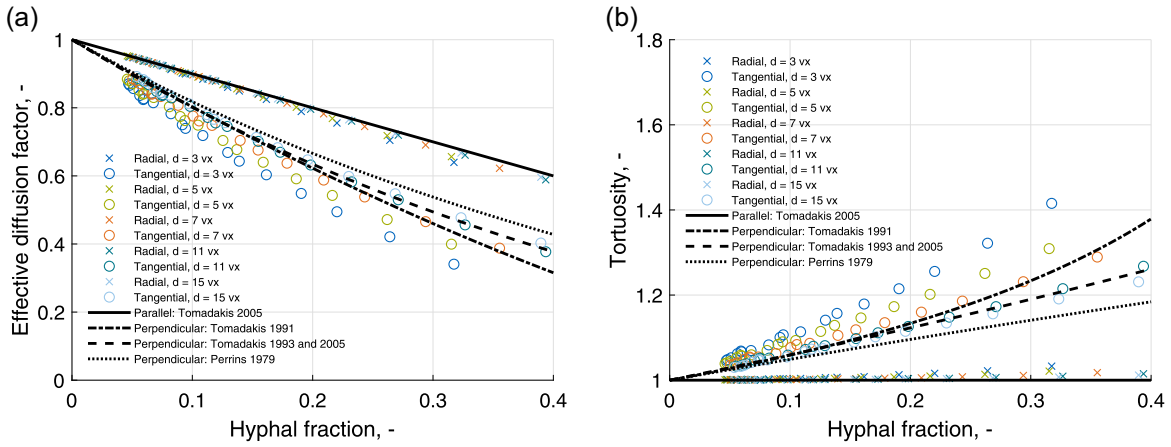

FIGURE 5 Diffusion computations of "Beam-Pellets" in the radial and tangential directions and comparison to existing literature correlations for parallel fibers (Table 1). The "Beam-Pellets" differ in the fiber-diameter in voxels, whereas the diameter in μm stayed constant (Figure 4). Each data point results from a single diffusion computation of a cubic sub-volume with a cube-edge length of 50 μm. Crosses and circles correspond to computed diffusion properties in the radial and tangential directions, respectively. The black lines represent literature correlations. The hyphal fraction corresponds to the ratio of the volume of hyphae to the total volume in the cubic sub-volumes [Color figure can be viewed at wileyonlinelibrary.com]

The results of the diffusion computations on the "Beam-Pellet" are shown in Figure 5 for the hyphal fraction range 0.05–0.4. A hyphal fraction of 0.4 was the maximum value for the *A. niger* pellets investigated in this study. Figure 5a shows the relation between the hyphal fraction of cubic sub-volumes and their corresponding effective diffusion factor. In the radial diffusion direction, the effective diffusion factor decreased almost linearly with increasing hyphal fractions. The radial effective diffusion factors showed a similar behavior as that of the often applied assumption for filamentous microorganisms: $k_{eff} = \epsilon$ (Buschulte, 1992; Celler et al., 2012; Silva et al., 2001; Van't Riet & Tramper, 1991). This formula is the prediction of the "law of mixtures" for the flow along parallel fibers (Tomadakis & Robertson, 2005). In the tangential directions, the effective diffusion factors were much smaller than their radial counterparts – and the slope was by no means in the order of minus one. Figure 5b shows the tortuosities for the radial and tangential diffusions, and it can be seen that they increase with increasing hyphal fractions. As expected, the tortuosities in the tangential diffusion direction were much higher than their radial counterparts.

To investigate the influence of the image resolution on the diffusion computations, we simulated "Beam-Pellets" with different resolutions (Section 2.5). With increasing resolutions, the effective diffusion factor increased and the tortuosity decreased, which was probably caused by the increased circularity of the filaments (Figure 4). As shown in Figure 3 and 4, representative cubes of the "Beam-Pellets" closely resemble parallel nonoverlapping fibers. Literature correlations for bulk diffusion through parallel fibers (Perrins et al., 1979; Tomadakis & Sotirchos, 1991, 1993; Tomadakis & Robertson, 2005) suggest, that the applied diffusion computations underestimate the diffusivity in the case of low resolutions. With increased resolutions, the computed diffusion results approach the literature correlations. However, it has to be mentioned that the literature correlations are for a square array of parallel fibers (Perrins et al., 1979), parallel random distributed overlapping fibers (Tomadakis & Sotirchos, 1991), and random distributed nonoverlapping fibers (Tomadakis & Robertson, 2005; Tomadakis & Sotirchos, 1993) and thus similar but not identical to our "Beam-Pellets."

In contrast to the tangential diffusion paths, the radial paths of the "Beam-Pellet" were not winding (Figure 3). In theory, increased path lengths result in an increased tortuosity and a decreased effective diffusion factor (Epstein, 1989). This behavior could be observed for the "Beam-Pellet" in the radial and tangential diffusion directions as well. The small difference between the computed radial effective diffusion factors/tortuosities and the "law of mixtures" for the flow along parallel fibers (Tomadakis & Robertson, 2005) $k_{eff} = \epsilon$ was evoked by the radial direction of the filaments of the "Beam-Pellet." Thus, the filaments were not completely parallel to each other. Further investigations with simulated perfectly parallel filaments resulted in $k_{eff} = \epsilon$ and a constant tortuosity of one (data now shown).

To sum up, the diffusion behavior of the "Beam-Pellet" was consistent with the diffusion theory described by Epstein (1989) and could be used to verify the applied diffusion computations. The comparison to literature correlations about the diffusivity of parallel fibers suggests that our diffusion computations of fibers with a low image resolution tend to underestimate the diffusivity, whereas high resolutions approach the literature correlations. The radial diffusion behavior of the "Beam-Pellet" illustrated the often applied literature assumption for filamentous microorganisms: $k_{eff} = \epsilon$ (Buschulte, 1992; Celler et al., 2012; Silva et al., 2001; Van't Riet & Tramper, 1991). However, the morphology of the idealized "Beam-Pellet" (Figure 3) was very different from the μCT data of *A. niger* pellets (Figure 2). Thus, the actual correlation between the effective diffusivity and the hyphal fraction of *A. niger* pellets was investigated in further detail.

3.2 | Effective diffusivity of *A. niger* pellets

Contrary to the "Beam-Pellet" (Figure 3), in the case of the *A. niger* pellets, the voids, that is, the spaces between the hyphae (Figure 2),

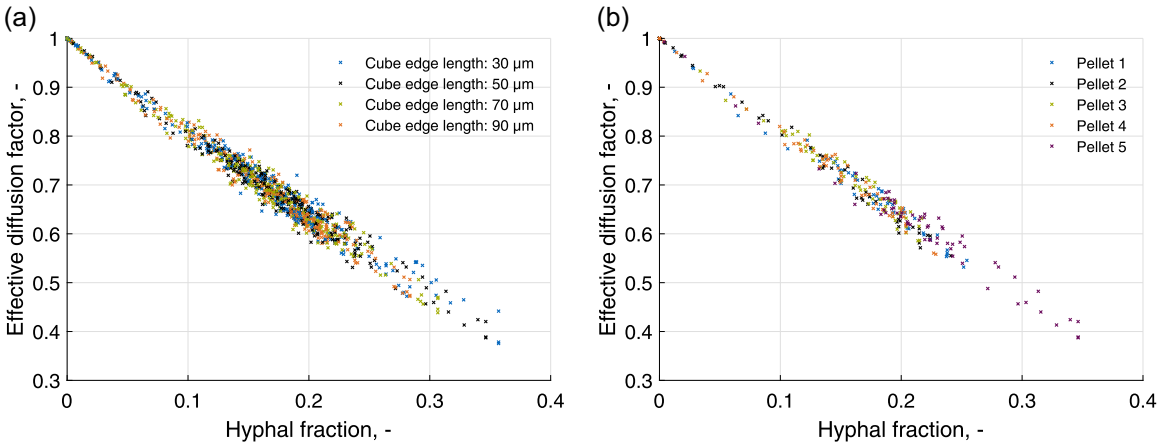

FIGURE 6 Correlations between the radial effective diffusion factor and hyphal fraction (ratio of the volume of hyphae to the total volume) for five *Aspergillus niger* pellets. Each data point results from a single diffusion computation of a cubic sub-volume: (a) Diffusion computations with different cube sizes. (b) The cube-edge length was 50 µm; each color represents the investigated cubes of one pellet [Color figure can be viewed at wileyonlinelibrary.com]

are strongly winded. According to Epstein (1989) that should result in an increased tortuosity, and therefore, in a decreased effective diffusivity. The tortuosity and effective diffusion factors of five *A. niger* pellets are investigated in this section. The diameters of the pellets were between 410 and 570 µm.

To investigate the influence of the size of the cubic sub-volumes on the diffusion computations, the edge length of the cubes was varied. Figure 6a shows the relation between the effective diffusion factor and the hyphal fraction for different cube sizes. The data include the diffusion computations of the five investigated *A. niger* pellets in the radial direction for cube-edge lengths of 30, 50, 70, and 90 µm. Generally, the effective diffusion factors for different cube-edge lengths showed similar behavior. When no hyphal material is present, that is, when the hyphal fraction is zero, the effective diffusion factor is one, and thus, the diffusion is not geometrically hindered. With increasing hyphal fraction, the effective diffusion factor decreases. The applied cube-edge lengths did not have a high impact on the diffusion results. Thus, a cube-edge length of 50 µm was applied for further computations in this study. Figure 6b) shows the effective diffusion factors of the five *A. niger* pellets studied herein for a cube-edge length of 50 µm. It can be seen that the values for the different pellets varied only slightly. As five pellets were investigated, this very subtle scattering of the data points implies that the method is quite reproducible when applied to different pellets obtained from the same cultivation sample.

Figure 7 shows the results of the diffusion computations for the five studied *A. niger* pellets in the radial and tangential directions for a cube-edge length of 50 µm. Figure 7a shows that the computed effective diffusion factors of the *A. niger* pellets were much smaller than the values expected from the literature assumption $k_{eff} = \epsilon$, and therefore, also much smaller than the values obtained for the investigated "Beam-Pellet." A slight anisotropy was observed when comparing the radial and tangential diffusion directions because the effective diffusion factors in the radial direction were slightly higher

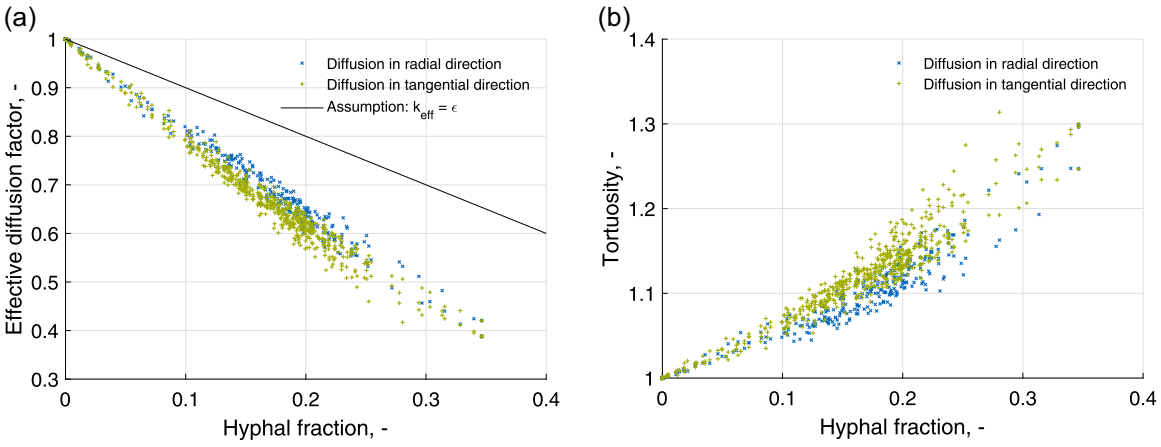

FIGURE 7 Diffusion computations of five *Aspergillus niger* pellets in the radial and tangential directions. Each data point results from a single diffusion computation of a cubic sub-volume with a cube-edge length of 50 µm; k_{eff} is the effective diffusion factor and ϵ is the porosity: (a) The blue and green data points correspond to effective diffusion factors in the radial and tangential directions, respectively; the black line represents the literature assumption $k_{eff} = \epsilon$. (b) The blue and green data points represent the tortuosities in the radial and tangential directions, respectively [Color figure can be viewed at wileyonlinelibrary.com]

than their counterparts in the tangential direction. In the absence of hyphal material, that is, when the hyphal fraction is zero, the tortuosity is one (Figure 7b). With increasing hyphal fraction, the tortuosity increases as well. Again, a slight difference was observed between the radial and tangential diffusion directions, with the radial diffusion computations resulting in lower tortuosities than their tangential counterparts. According to Equation (2), the lower tortuosities explain the higher effective diffusion factors in the radial direction. In the model assumption $k_{eff} = -c_h + 1 = \epsilon$, the tortuosity is assumed to be constantly one. This simplification explains the differences between our computed effective diffusion factors for the *A. niger* pellets and the values expected from the literature (Figure 7a) as well as those reported for the "Beam-Pellet" in the previous section.

The local hyphal fraction range of the five investigated *A. niger* pellets was 0–0.4. To the best of our knowledge, there are no reports in the literature, in which the hyphal fraction of filamentous pellets is higher than the maximum hyphal fraction measured in this study, for example, Cui, Van der Lans, and Luyben (1997, 1998) reported average hyphal fractions between 0.07 and 0.30 for whole *Aspergillus awamori* pellets. Thus, the hyphal fraction ranges of the investigated *A. niger* pellets could already be representative for realistic pellets.

3.3 | Correlation between effective diffusivity and hyphal fraction

The diffusion computations of the five investigated *A. niger* pellets (Section 3.2) are compared to literature assumptions (Table 1) for the correlation between the effective diffusion factor (k_{eff}) and the hyphal fraction (c_h)/solid fraction/porosity ($\epsilon = 1 - c_h$) of filamentous microorganisms (Figure 8a) and fibers (Figure 8b). As the diffusion of spherical pellets should be driven mainly by radial diffusion, we have investigated it herein. Additionally, a new modeling approach was introduced to correlate the effective diffusion factor and the hyphal fraction.

The computed diffusion factors differed strongly from the assumption $k_{eff} = \epsilon$, which has been used for simulation/modeling studies of filamentous microorganisms by Celler et al. (2012), Buschulte (1992), and Silva et al. (2001). In fact, the computed effective diffusion factors were far below the expected values. In those previous models, the effective diffusion factor was assumed to be only dependent on the porosity of the material, while neglecting the tortuosity. Thus, the difference between our computed effective diffusion factors and previous assumptions (Buschulte, 1992; Celler et al., 2012; Silva et al., 2001) was not surprising. The second linear literature assumption for filamentous microorganisms was $k_{eff} = \epsilon/2$ (Lejeune & Baron, 1997). In their work, Lejeune and Baron (1997) considered the tortuosity to be consistently 2, without explaining that assumption. As shown, their model differed strongly from the computed data. Their model would result in a geometrically hindered diffusion for a hyphal fraction of zero. Thus, especially for low hyphal fractions, that assumption seems to be untenable. In their growth modeling approach for filamentous microorganisms, Meyerhoff et al. (1995) applied a nonlinear correlation between the effective diffusion factor and the hyphal fraction: $k_{eff} = (2 - c_h)/(2 + c_h)$. This approach seemed to approximate our computed data better than the two previous model assumptions from the literature. Additionally, the effective diffusion factor is 1 and 0 for hyphal fractions of 0 and 1, respectively. In theory, these conditions should be fulfilled. However, the model seemed to overestimate the effective diffusion factors. Besides the assumption $k_{eff} = \epsilon$, Buschulte (1992) deduced a second model for filamentous microorganisms: $k_{eff} = e^{-2.8c_h}$. In comparison with the other literature assumptions for filamentous microorganisms, this approach fitted our computed data best. However, in the hyphal fraction range of 0–0.4, the model seemed to underestimate the computed data. Additionally, for a hyphal fraction of 1, the model would result in an effective diffusion factor of

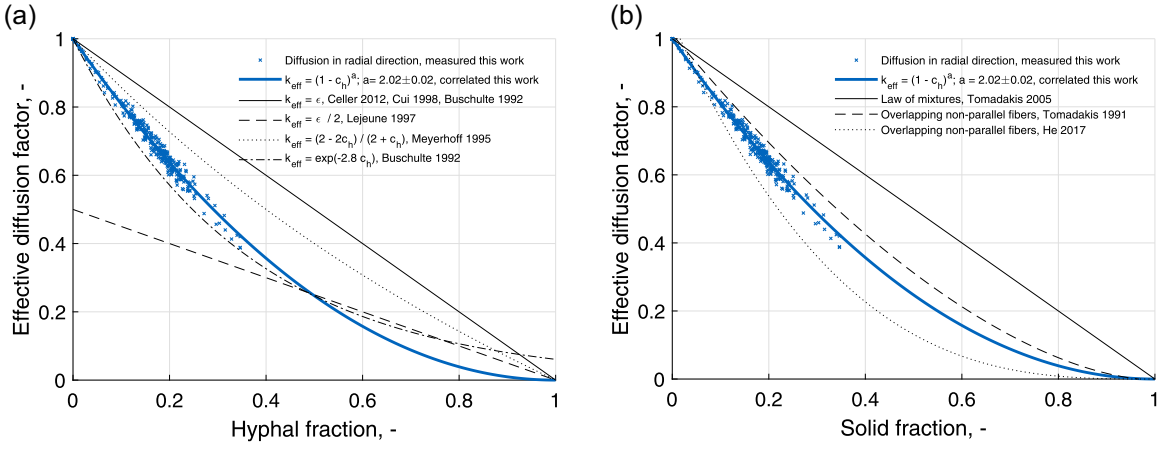

FIGURE 8 Correlations between hyphal fraction (c_h)/solid fraction/porosity ($\epsilon = 1 - c_h$) and effective diffusion factor (k_{eff}). The blue data points correspond to the computed effective diffusion factors of five *Aspergillus niger* pellets in the radial direction, with the cube-edge length for the diffusion calculations being 50 μm. The solid bold blue line shows the new correlation between the hyphal fraction and the effective diffusion factor; the black lines represent existing correlations in the literature (Table 1) for (a) filamentous microorganisms and (b) 3D random distributed overlapping fibers [Color figure can be viewed at wileyonlinelibrary.com]

0.06. In theory, for a hyphal fraction of 1, the effective diffusion factor has to be 0 (Epstein, 1989).

The correlations for 3D random distributed overlapping fibers (Figure 8b) fitted our data better than the correlations existing for filamentous microorganisms. Our data fall in between the correlation of Tomadakis and Sotirchos (1991) and He et al. (2017). In both studies, the computation of the effective diffusivity was well validated for other structures like parallel fibers. However, they differ significantly. Tomadakis and Sotirchos (1991) applied a modification of Archie's law (Archie, 1942) to correlate the tortuosity factor $\tau^2 = ((1 - \epsilon_p)/(\epsilon - \epsilon_p))^{\alpha}$, with the percolation porosity $\epsilon_p = 0.037$ and $\alpha = .661$. It has to be mentioned that the modification of Archie's law also fitted well for Vignoles et al. (2007) for bulk diffusion of μCT-generated images of parallel fibrous carbon-carbon composite preforms. The percolation porosity was $\epsilon_p = 0.04$ and $\alpha = 0.107/\alpha = 0.465$ for diffusion parallel/perpendicular to the fibers, respectively. According to Nam and Kaviany (2003), the effective diffusivity of isotropic structures is often estimated using a power function of porosity. Thus, He et al. (2017) fitted their diffusion results of 3D random distributed overlapping fibers and found $k_{eff} = \alpha\epsilon^n$, with $\alpha = 1.05$ and $n = 3$.

To overcome the limitations and/or inaccuracies in the correlations between the effective diffusion factor and hyphal fraction for filamentous microorganisms and to obtain a relation with only one fitting parameter, we propose a new correlation:

$$k_{eff} = (1 - c_h)^a, \tag{4}$$

where a is the only fitting parameter. This rather simple expression guarantees theory-consistent effective diffusion factors of 1 and 0 at hyphal fractions of 0 and 1, respectively, and provides an excellent fit to our data. Minimizing the error squares, $a = 2.02 \pm 0.02$ (with 95% confidence bounds):

$$k_{eff} = (1 - c_h)^{2.02 \pm 0.02}. \tag{5}$$

In conclusion, the literature assumptions for modeling diffusion in filamentous pellets failed to fit our computed results, whereas correlations for fibers in material science fitted our data better. Thus, we set up a nonlinear equation (5) approach with only one fitting parameter, which is a special case for the power function of porosity, for $\alpha = 1$ as well as for the modified Archie's law, when $\epsilon_p = 0$. This approach modeled the correlation between the effective diffusion factor and the hyphal fraction for five investigated *A. niger* pellets quite well.

3.4 | Proposed workflow in bioprocess development

Depending on the product of interest, a saturation or a limitation of substrates inside fungal pellets is pursued (Veiter et al., 2018). To predict the spatial distribution of substrates inside pellets, the effective diffusivity through the fibrous network has to be known (Buschulte, 1992; Celler et al., 2012). Thus, our newly proposed method to determine the effective diffusivity of filamentous fungal pellets with μCT measurements and subsequent diffusion computations through the three-dimensional morphology has considerable benefits for bioprocess development. We propose the following idealized workflow to achieve an optimal/suitable pellet morphology:

(1) Generate pellets through experiments or simulations
   a) Cultivate different strains at different process conditions; apply μCT measurements and subsequent image analysis of pellets (Schmideder et al., 2019)
   b) Simulate various three-dimensional pellet-networks with algorithms similar to Celler et al. (2012); model calibration could be carried out based on μCT measurements with subsequent image analysis (Schmideder et al., 2019)
(2) Compute the correlation between the hyphal fraction and the effective diffusivity for each existing and simulated pellet of Step 1, as described in the present study
(3) Compute the proportion of substrate-limited and substrate-saturated regions of each pellet based on the consumption- and diffusion-terms of models such as Buschulte (1992)); apply correlation of the hyphal fraction and effective diffusivity in diffusion terms (this study; Step 2)
(4) Assemble data base of experimentally or simulatively generated pellets including substrate-supply and morphological features
(5) Select optimal/suitable pellet for the desired process from data base
(6) Realize optimal/suitable pellet in bioprocess, for example, through the upscale of previous experiments (Step 1a), genetic modifications, or process control

Obviously, some of these steps have to be investigated and elaborated in much more detail to reach the proposed optimum macromorphology through this workflow. However, we consider the investigation of the effective diffusivity as an important step towards morphological engineering. In our study, we investigated five pellets of one process and the correlation between the effective diffusivity and hyphal fraction scattered only slightly. Thus, we propose, that our method is at least reproducible for a certain strain at certain process conditions. If the observed correlation between the hyphal fraction and the effective diffusivity is representative for the applied *A. niger* strain in general, other fungal strains, and/or theoretically all filamentous microorganisms should be the focus of future studies. Thereby, as described, μCT measurements are suitable to detect the three-dimensional morphology used for diffusion computations. However, other three-dimensional methods such as confocal laser scanning microscopy of pellets slices or even simulated pellets are also conceivable to explore other strains and processes.

4 | CONCLUSIONS

The findings described in this manuscript unveil the actual relation between the hyphal fraction (c_h, i.e., the ratio between the volume of

hyphae and the total volume) and the effective diffusion factor (k_{eff}) and tortuosity inside filamentous fungal pellets. They also uncover a discrepancy with the assumptions made in the literature for filamentous microorganisms so far. We propose a new correlation, which is inspired by correlations for fibers, rather simple, consistent with theoretical expectations, and shows an excellent fit to the investigated *A. niger* pellets: keff=$(1 - c_h)^2$. Our μCT images resulted in hyphae with a diameter of approximately five voxels. As indicated in Section 3.1 and Figure 5, that might lead to a slight underestimation of the diffusivity. For future studies of fibers/filamentous microorganisms, we recommend μCTs, that could resolve fibers/hyphae to a diameter of approximate 11 voxels. Alternatively, a correction factor could be calculated based on diffusion computations of simulated filamentous pellets. The method described in this study is not limited to *A. niger* but can also be applied to a variety of fungal species as well as to other organisms forming filamentous structures. It is conceivable to use the described workflow not only based on μCT data, but also on other three-dimensional data such as confocal laser scanning microscopy (CLSM) images of smaller structures and pellet slices, or even simulated pellets. The computed diffusion parameters, and thus the diffusion rates of substrates and products inside fungal pellets, could in combination with a consumption and production model, be applied to predict the actual metabolic flux inside filamentous pellets. With this information, it would be possible to propose an ideal fungal macromorphology for the production of a certain substance, which could then be achieved by genetic engineering and control of the process parameters during fermentation.

ACKNOWLEDGMENTS

The authors want to thank Markus Betz and Christian Preischl for preliminary studies on diffusion computations of filamentous pellets and Clarissa Schulze for assistance with μCT measurements. We also wish to thank Christoph Kirse and Michael Kuhn for helpful discussions about diffusion mechanisms. This study made use of equipment that was funded by the Deutsche Forschungsgemeinschaft (DFG, German Research Foundation)–198187031. The authors thank the Deutsche Forschungsgemeinschaft for financial support for this study within the SPP 1934 DiSPBiotech–315384307 and 315305620.

CONFLICT OF INTERESTS

The authors declare that there is no conflict of interests.

ORCID

Stefan Schmideder http://orcid.org/0000-0003-4328-9724
Lars Barthel http://orcid.org/0000-0001-8951-5614
Henri Müller http://orcid.org/0000-0002-4831-0003
Vera Meyer http://orcid.org/0000-0002-2298-2258
Heiko Briesen http://orcid.org/0000-0001-7725-5907

REFERENCES

Archie, G. E. (1942). The electrical resistivity log as an aid in determining some reservoir characteristics. *Transactions of the AIME*, *146*(01), 54–62. https://doi.org/10.2118/942054-g

Aris, R. (1975). *The mathematical theory of diffusion and reaction in permeable catalysts*. Clarendon Press.

Becker, J., Wieser, C., Fell, S., & Steiner, K. (2011). A multi-scale approach to material modeling of fuel cell diffusion media. *International Journal of Heat and Mass Transfer*, *54*(7-8), 1360–1368. https://doi.org/10.1016/j.ijheatmasstransfer.2010.12.003

Brakhage, A. A. (2013). Regulation of fungal secondary metabolism. *Nature Reviews Microbiology*, *11*(1), 21. https://doi.org/10.1038/nrmicro2916

Buschulte, T. K. (1992). *Mathematische Modellbildung und Simulation von Zellwachstum, Stofftransport und Stoffwechsel in Pellets aus Streptomyceten*. PhD thesis, Fakultät Verfahrenstechnik der Universität Stuttgart.

Cairns, T. C., Zheng, X., Zheng, P., Sun, J., & Meyer, V. (2019). Moulding the mould: Understanding and reprogramming filamentous fungal growth and morphogenesis for next generation cell factories. *Biotechnology for Biofuels*, *12*(1), 77. https://doi.org/10.1186/s13068-019-1400-4

Celler, K., Picioreanu, C., van Loosdrecht, M. C., & van Wezel, G. P. (2012). Structured morphological modeling as a framework for rational strain design of streptomyces species. *Antonie Van Leeuwenhoek*, *102*(3), 409–423.

Coindreau, O., Mulat, C., Germain, C., Lachaud, J., & Vignoles, G. L. (2011). Benefits of x-ray cmt for the modeling of c/c composites. *Advanced Engineering Materials*, *13*(3), 178–185. https://doi.org/10.1002/adem.201000233

Colin, V. L., Baigorí, M. D., & Pera, L. M. (2013). Tailoring fungal morphology of *Aspergillus niger* MYA 135 by altering the hyphal morphology and the conidia adhesion capacity: Biotechnological applications. *AMB Express*, *3*, 27. https://doi.org/10.1186/2191-0855-3-27

Cui, Y., Van der Lans, R., Luyben, K., et al. (1997). Effect of agitation intensities on fungal morphology of submerged fermentation. *Biotechnology and Bioengineering*, *55*(5), 715–726.

Cui, Y., Van der Lans, R., Luyben, K., et al. (1998). Effects of dissolved oxygen tension and mechanical forces on fungal morphology in submerged fermentation. *Biotechnology and Bioengineering*, *57*(4), 409–419.

Epstein, N. (1989). On tortuosity and the tortuosity factor in flow and diffusion through porous media. *Chemical Engineering Science*, *44*(3), 777–779. https://doi.org/10.1016/0009-2509(89)85053-5

Fiedler, M. R., Barthel, L., Kubisch, C., Nai, C., & Meyer, V. (2018). Construction of an improved *Aspergillus niger* platform for enhanced glucoamylase secretion. *Microbial Cell Factories*, *17*, 95. https://doi.org/10.1186/s12934-018-0941-8

Foerst, P., de Carvalho, T. M., Lechner, M., Kovacevic, T., Kim, S., Kirse, C., & Briesen, H. (2019). Estimation of mass transfer rate and primary drying times during freeze-drying of frozen maltodextrin solutions based on x-ray μ-computed tomography measurements of pore size distributions. *Journal of Food Engineering*, https://doi.org/10.1016/j.jfoodeng.2019.05.002

Gabitto, J., & Tsouris, C. (2017). Surface transport processes in charged porous media. *Journal of Colloid and Interface Science*, *498*, 91–104. https://doi.org/10.1016/j.jcis.2017.03.009

Gorski, K. M., Hivon, E., Banday, A., Wandelt, B. D., Hansen, F. K., Reinecke, M., & Bartelmann, M. (2005). Healpix: A framework for high-resolution discretization and fast analysis of data distributed on the sphere. *The Astrophysical Journal*, *622*, 759. https://doi.org/10.1086/apj.2005.622.issue-2

He, X., Guo, Y., Li, M., Pan, N., & Wang, M. (2017). Effective gas diffusion coefficient in fibrous materials by mesoscopic modeling. *International*

Journal of Heat and Mass Transfer, *107*, 736–746. https://doi.org/10.1016/j.ijheatmasstransfer.2016.11.097

Hille, A., Neu, T., Hempel, D., & Horn, H. (2009). Effective diffusivities and mass fluxes in fungal biopellets. *Biotechnology and Bloengineering*, *103*(6), 1202–1213.

Lejeune, R., & Baron, G. V. (1997). Simulation of growth of a filamentous fungus in 3 dimensions. *Biotechnology and Bioengineering*, *53*, 139–150. https://doi.org/10.1002/(sici)1097-0290(19970120)53:2<139::aid-bit3>3.3.co;2-e

Medveď, I., & Černý, R. (2011). Surface diffusion in porous media: A critical review. *Microporous and Mesoporous Materials*, *142*(2-3), 405–422. https://doi.org/10.1016/j.micromeso.2011.01.015

Meyer, V. (2008). Genetic engineering of filamentous fungi: Progress, obstacles and future trends. *Biotechnology Advances*, *26*, 177–185. https://doi.org/10.1016/j.biotechadv.2007.12.001

Meyer, V., Andersen, M. R., Brakhage, A. A., Braus, G. H., Caddick, M. X., Cairns, T. C., & Head, R. M. (2016). Current challenges of research on filamentous fungi in relation to human welfare and a sustainable bio-economy: A white paper. *Fungal Biology and Biotechnology*, *3*, 6. https://doi.org/10.1186/s40694-016-0024-8

Meyerhoff, J., Tiller, V., & Bellgardt, K.-H. (1995). Two mathematical models for the development of a single microbial pellet; part 1: Detailed morphological model based on the description of individual hyphae. *Bioprocess Engineering*, *12*(6), 305–313.

Miyabe, K., & Guiochon, G. (2010). Surface diffusion in reversed-phase liquid chromatography. *Journal of Chromatography A*, *1217*(11), 1713–1734. https://doi.org/10.1016/j.chroma.2009.12.054

Nam, J. H., & Kaviany, M. (2003). Effective diffusivity and water-saturation distribution in single-and two-layer pemfc diffusion medium. *International Journal of Heat and Mass Transfer*, *46*(24), 4595–4611. https://doi.org/10.1016/S0017-9310(03)00305-3

Neale, G. H., & Nader, W. K. (1973). Prediction of transport processes within porous media: Diffusive flow processes within an homogeneous swarm of spherical particles. *AIChE Journal*, *19*(1), 112–119. https://doi.org/10.1002/aic.690190116

Nielsen, J. (1993). A simple morphologically structured model describing the growth of filamentous microorganisms. *Biotechnology and Bioengineering*, *41*, 715–727. https://doi.org/10.1002/bit.260410706

Otsu, N. (1979). A threshold selection method from gray-level histograms. *IEEE Transactions on Systems, Man, and Cybernetics*, *9*, 62–66. https://doi.org/10.1109/tsmc.1979.4310076

Panerai, F., Ferguson, J. C., Lachaud, J., Martin, A., Gasch, M. J., & Mansour, N. N. (2017). Micro-tomography based analysis of thermal conductivity, diffusivity and oxidation behavior of rigid and flexible fibrous insulators. *International Journal of Heat and Mass Transfer*, *108*, 801–811. https://doi.org/10.1016/j.ijheatmasstransfer.2016.12.048

Papagianni, M. (2004). Fungal morphology and metabolite production in submerged mycelial processes. *Biotechnology advances*, *22*(3), 189–259.

Perrins, W., McKenzie, D. R., & McPhedran, R. (1979). Transport properties of regular arrays of cylinders. *Proceedings of the Royal Society of London. A. Mathematical and Physical Sciences*, *369*(1737), 207–225. https://doi.org/10.1098/rspa.1979.0160

Pirt, S. (1966). A theory of the mode of growth of fungi in the form of pellets in submerged culture. *Proceedings of the Royal Society of London*, *166*, 369–373. https://doi.org/10.1098/rspb.1966.0105

Schmideder, S., Barthel, L., Friedrich, T., Thalhammer, M., Kovačević, T., Niessen, L., & Briesen, H. (2019). An x-ray microtomography-based method for detailed analysis of the three-dimensional morphology of fungal pellets. *Biotechnology and Bioengineering*, https://doi.org/10.1002/bit.26956

Silva, E. M. E., Gutierrez, G. F., Dendooven, L., Hugo, J. I., & Ochoa-Tapia, J. A. (2001). A method to evaluate the isothermal effectiveness factor for dynamic oxygen into mycelial pellets in submerged cultures. *Biotechnology Progress*, *17*(1), 95–103. https://doi.org/10.1021/bp0001361

Tomadakis, M. M., & Robertson, T. J. (2005). Viscous permeability of random fiber structures: Comparison of electrical and diffusional estimates with experimental and analytical results. *Journal of Composite Materials*, *39*(2), 163–188. https://doi.org/10.1177/0021998305046438

Tomadakis, M. M., & Sotirchos, S. V. (1991). Effects of fiber orientation and overlapping on knudsen, transition, and ordinary regime diffusion in fibrous substrates. *MRS Online Proceedings Library Archive*, *250*, https://doi.org/10.1557/proc-250-221

Tomadakis, M. M., & Sotirchos, S. V. (1993). Effective diffusivities and conductivities of random dispersions of nonoverlapping and partially overlapping unidirectional fibers. *The Journal of chemical physics*, *99*(12), 9820–9827. https://doi.org/10.1063/1.465464

Van't Riet, K., & Tramper, J. (1991). *Basic bioreactor design*. CRC Press.

Veiter, L., Rajamanickam, V., & Herwig, C. (2018). The filamentous fungal pellet: Relationship between morphology and productivity. *Applied Microbiology and Biotechnology*, 1–10. https://doi.org/10.1007/s00253-018-8818-7

Velichko, A., Wiegmann, A., & Mücklich, F. (2009). Estimation of the effective conductivities of complex cast iron microstructures using fib-tomographic analysis. *Acta Materialia*, *57*(17), 5023–5035. https://doi.org/10.1016/j.actamat.2009.07.004

Vignoles, G. L., Coindreau, O., Ahmadi, A., & Bernard, D. (2007). Assessment of geometrical and transport properties of a fibrous c/c composite preform as digitized by x-ray computerized microtomography: Part ii. heat and gas transport properties. *Journal of materials research*, *22*(6), 1537–1550. https://doi.org/10.1557/jmr.2007.0216

Vorlop, K.-D. (1984). *Entwicklung von Verfahren zur Polymerfixierung von Mikroorganismen und Anwendung der Biokatalysatoren zur Spaltung von Penicillin G und Synthese von L-Tryptophan*. PhD thesis, Naturwissenschaftliche Fakultät der Technischen Universität Carolo-Wilhemina zu Braunschweig.

Wiegmann, A., & Zemitis, A. (2006). *EJ-HEAT: A fast explicit jump harmonic averaging solver for the effective heat conductivity of composite materials*. Fraunhofer Institute ITWM.

Wittier, R., Baumgartl, H., Lübbers, D. W., & Schügerl, K. (1986). Investigations of oxygen transfer into Penicillium chrysogenum pellets by microprobe measurements. *Biotechnology and Bioengineering*, *28*(7), 1024–1036. https://doi.org/10.1002/bit.260280713

Yaws, C. L. (2014). *Transport properties of chemicals and hydrocarbons*. William Andrew.

How to cite this article: Schmideder S, Barthel L, Müller H, Meyer V, Briesen H. From three-dimensional morphology to effective diffusivity in filamentous fungal pellets. *Biotechnology and Bioengineering*. 2019;116:3360–3371. https://doi.org/10.1002/bit.27166